

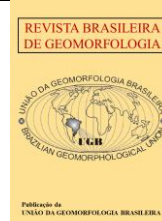


<https://rbgeomorfologia.org.br/>
ISSN 2236-5664

Revista Brasileira de Geomorfologia

v. 26, n° 2 (2025)

<http://dx.doi.org/10.20502/rbg.v26i2.2599>



Research Article

Morphological changes in the lower estuarine coastal sector and socio-environmental impacts – Amapá: between 1992 and 2022

Mudanças morfológicas no Baixo Setor Costeiro Estuarino e Impactos Socioambientais – Amapá: entre 1992 e 2022

Maxwell Moreira Baia ¹, Orleno Marques da Silva Junior ²

¹ Federal University of Amapá - UNIFAP, Department of Postgraduate Studies in Geography, Macapá-AP, Brazil. E-mail: maxwmoreirabaia.mmb@gmail.com. ORCID: <https://orcid.org/0000-0001-8000-5634>

² Federal University of Amapá - UNIFAP, Department of Postgraduate Studies in Geography, Macapá-AP, Brazil. E-mail: orleno@ppe.ufrj.br. ORCID: <https://orcid.org/0000-0002-1173-1429>

Recebido: 17/07/2024; Aceito: 18/02/2025; Publicado: 19/05/2025

Abstract: Coastal regions are transitional areas between terrestrial and marine environments, with dynamic ecosystems, high biodiversity, economic productivity, population density and environmental fragility. The Amapá Coastal Zone is 800 km long and is influenced by atmospheric and oceanographic agents as well as the Amazon River. The study examined the variation between erosion and accretionary processes and their consequences, such as loss of infrastructure, lack of energy and increased saline intrusion in communities between the Gurijuba and Araguari rivers, including the Bailique archipelago. The physiographic characteristics, fieldwork and a multi-temporal series between the years 1992, 2005, 2014 and 2022 were analyzed. It was identified that 60% of the area presents accretion processes, represented by the formation of muddy banks, tidal flats and the clogging of the mouth of the Araguari River, while 40% suffers erosion, affecting 14 of the 20 monitored communities, highlighting the opening of drainages and modification of hydrodynamics. The deficiency in the management of these modifications has generated isolated and ineffective mitigating actions, aggravating the effects of erosion and wasting resources. If current trends are maintained, including forecasts of increased extreme weather events and sea level, more losses will occur, causing irreversible changes in local morphology and hydrodynamics in the short term.

Keywords: Amapá Coast; Erosion; Amazon River; Bailique Archipelago; Monitoring.

Resumo: As regiões costeiras são áreas de transição entre ambientes terrestres e marinhos, com ecossistemas dinâmicos, grande biodiversidade, produtividade econômica, densidade populacional e fragilidade ambiental. A Zona Costeira Amapaense apresenta 800 km de extensão, é influenciada por agentes atmosféricos, oceanográficos e pelo rio Amazonas. O estudo examinou a variação entre processos erosivos e acrescionários e suas consequências, como perda de infraestrutura, falta de energia e aumento da intrusão salina em comunidades entre os rios Gurijuba e Araguari, incluindo o arquipélago do Bailique. Analisou-se as características fisiográficas, trabalhos de campo e uma série multitemporal entre os anos 1992, 2005, 2014 e 2022. Identificou-se que 60% da área apresenta processos de acreção, representados pela formação de bancos lamosos, planícies de maré e a colmatção da foz do rio Araguari, enquanto 40% sofre erosão, afetando 14 das 20 comunidades monitoradas, destaque para abertura de drenagens e modificação da hidrodinâmica. A deficiência na gestão dessas modificações tem gerado ações mitigadoras isoladas e ineficazes, agravando os efeitos da erosão e desperdiçando recursos, caso as tendências atuais sejam mantidas, incluindo previsões de aumento de eventos climáticos extremos e do nível do mar, mais perdas ocorrerão, causando mudanças irreversíveis na morfologia e na hidrodinâmica local, em curto prazo.

Palavras-chave: Costa do Amapá; Erosão; Rio Amazonas; Arquipélago do Bailique; Monitoramento

1. Introduction

In recent decades, human activities have become the primary modifying agent of the environment, interfering with other agents and accelerating broader and more effective transformations in spatial organization. In coastal regions, these transformations often surpass the natural systems' resilience capacity, destroying environmental functions and jeopardizing the socio-economic and environmental sustainability of populations (COSTA e SOUZA, 2009; WATERS et al., 2016).

These areas connect terrestrial and marine environments, where the hydrosphere, lithosphere, atmosphere, biosphere, and human society interact frequently on different temporal scales. These environments host complex, dynamic ecosystems with high fragility, significant biodiversity, productivity, population density, and economic activities. They rank among the most vulnerable areas to climate change (CROSSLAND et al., 2005; NICHOLLS et al., 2007; MUEHE, 2012; DETHIER; HARPER, 2011; MENTASCHI et al., 2018; AUCELLI et al., 2018; CHEN et al., 2023).

Brazil has one of the world's most extensive coastal zones, with approximately 9,200 km of coastline bordering the Atlantic Ocean (VILLWOCK et al., 2005). The terrestrial strip encompasses over 400 municipalities across 17 states, with about 111.28 million people living within 150 kilometers of the coast, representing 54.8% of the total population (IBGE, 2022).

The Amazonian portion accounts for 35% of Brazil's coastline, extending 2,250 km across the states of Amapá, Pará, and Maranhão. This region is characterized by high freshwater discharge, particulate and sediment deposition, atmospheric and oceanic currents, and diverse environments such as estuaries, mangroves, tidal flats, swamps, beaches, floodplain forests, islands, deltas, dunes, sandbanks, and protected areas. Activities include livestock farming, mining, fishing, and tourism. These features contribute to the area's high morphological sensitivity and instability, which drive changes in coastal environments and the evolution of the area (SOUZA FILHO et al., 2011; PEREIRA et al., 2012; MARENGO, 2016; PRESTES, SILVA e JEANDE, 2018; RODRIGUES e SILVA JUNIOR, 2021).

As a subsystem of the Amazonian coastal zone, the Amapá coastal zone stretches approximately 800 km between the mouths of the Jarí and Oiapoque rivers. It is divided into estuarine and oceanic sectors and comprises an extensive plain covering portions of 11 of the state's 16 municipalities. This area is marked by dynamic interactions among atmospheric, oceanographic, and sediment dispersion agents from the Amazon River, leading to modifications on a relatively short temporal scale compared to other environments (TORRES, EL-ROBRINI e COSTA, 2018; ANTHONY et al., 2021; SILVA JUNIOR, SZLAFSZTEIN e BAIA, 2022).

These modifications are governed by the interactive action of tidal processes, waves, and winds, causing erosion, transport, sedimentation, and seasonal shifts in coastlines. These changes reflect an integrated response to the coast's behavior under dynamic processes and agents (SANTOS et al., 2018; SILVA JUNIOR, SANTOS e RODRIGUES, 2020; ANTHONY et al., 2021).

This study aims to analyze variations in erosive and accretion dynamics and their socio-environmental impacts on local communities. A semi-quantitative methodology was applied, integrating natural agents and anthropogenic factors as spatial parameters influencing coastal erosion processes. A multi-temporal analysis was conducted for 1992, 2005, 2014, and 2022, utilizing remote sensing data and geoprocessing techniques in a GIS environment.

2. Study Area

The area studied is located in the lower estuarine coastal sector, east of Amapá state, between the mouths of the Gurijuba and Araguari rivers, including the Bailique Archipelago. It encompasses a perimeter of 2,600 km², with a population of over 10,000 residents and more than 52 communities (IBGE, 2022). The local economy is based on fishing, extraction, and buffalo farming. Access is primarily via the Northern Canal of the Amazon River, covering a 180-kilometer route from Macapá (Figure 1).

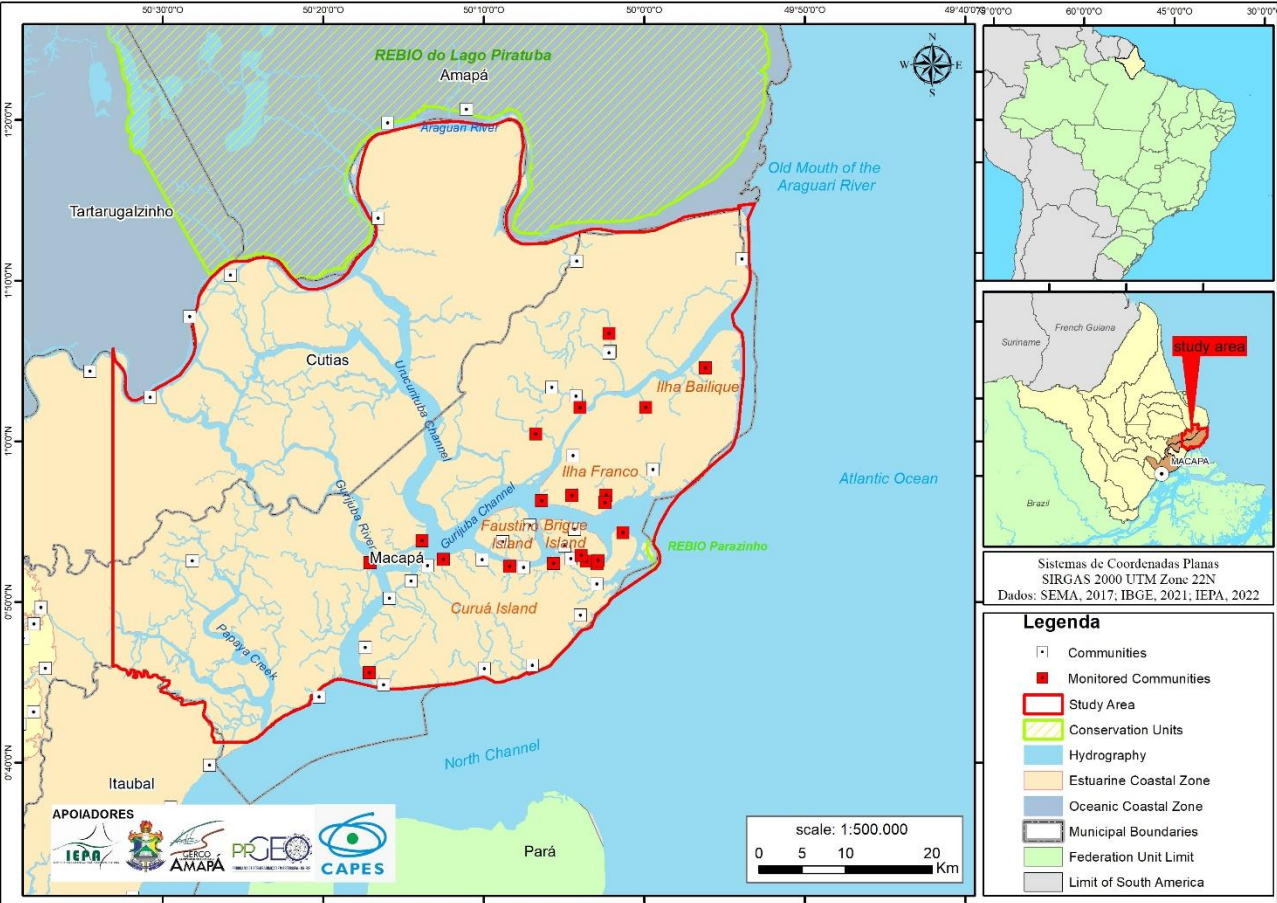
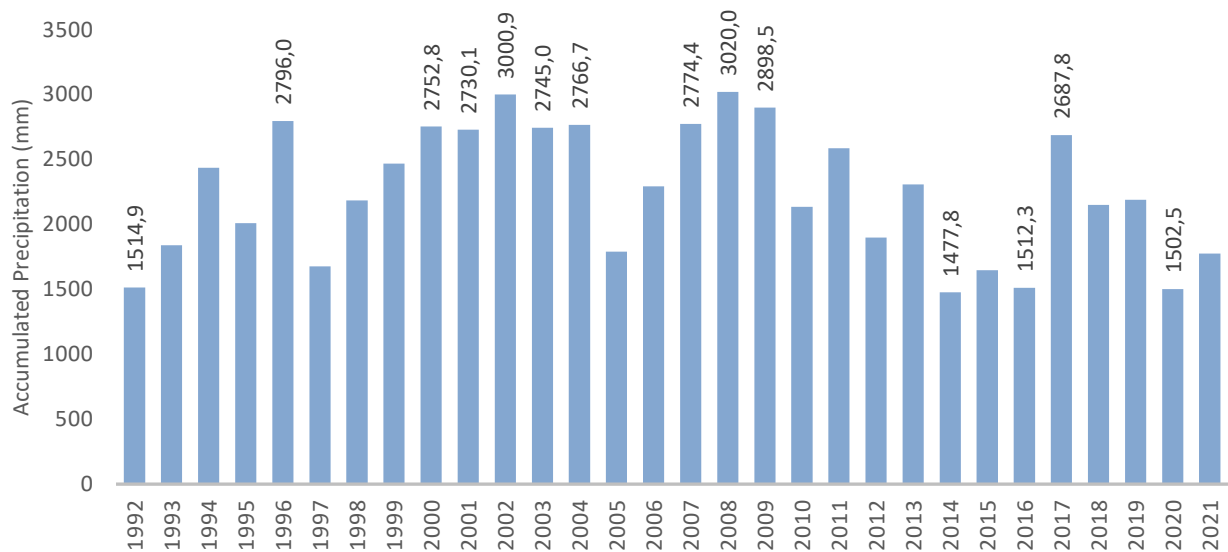


Figure 1. The area studied.

This region exhibits significant variation in annual precipitation. Estimates from the Climate Hazards Group InfraRed Precipitation with Stations (CHIRPS) sensor for 1992 to 2022 indicate accumulated rainfall exceeding 2,600 mm, with minimum values below 1,600 mm and an annual average of 2,470.73 mm. The mean annual temperature is 27°C (Graph 1). Isohyets show monthly precipitation exceeding 400 mm in March and April and falling below 200 mm during the peak dry season in September, October, and November.



Graph 1. Estimate of accumulated annual precipitation for the study area.

The area comprises a very low, flat coastal plain characterized by fluviolacustrine and fluviomarine environments, with alluvial deposits, Pleistocene terraces, and Holocene deposits (TORRES, EL-ROBRINI e COSTA, 2018). The soil profile includes suborders of Gleysols (Thionic, Melanic, and Haplic), typical of flooded areas or those subject to tidal oscillation. These hydromorphic soils are poorly developed, highly acidic, and rich in organic matter and soluble salts (IBGE, 2017).

Vegetation cover consists of alluvial Ombrophilous Forest and Pioneer Formations. Alluvial formations are concentrated near rivers, extending into the fluviomarine plains. Pioneer formations develop in pedologically unstable areas with constant sediment deposition, predominantly featuring *Avicennia germinans*, *Rhizophora harrisonii*, and *Rhizophora mangle* (COSTA NETO e SILVA, 2004).

2. Materials and Method

For mapping variations in erosive and accretion dynamics, the methodological propositions are anchored in an integrated environmental analysis of natural components, anthropogenic activities, and geoprocessing techniques. The study was divided into four axes: 1) Data Acquisition, 2) Characterization, 3) Processing, and 4) Integration of Results (Figure 2).

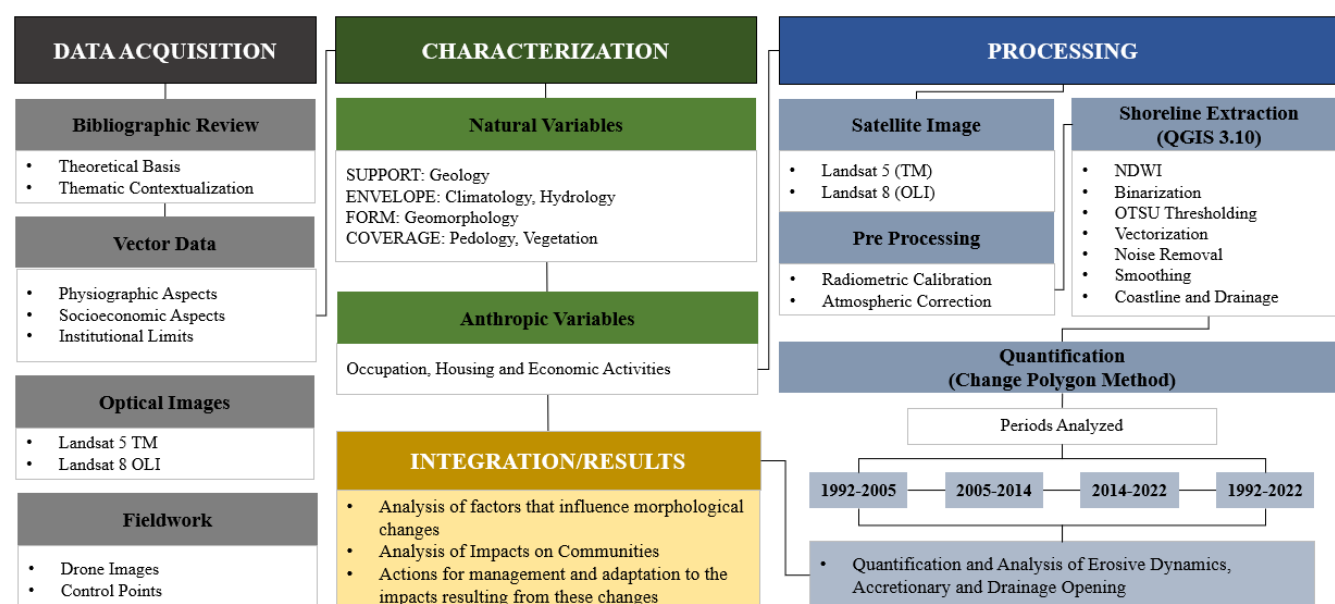


Figure 2. Methodological Flowchart Source: Prepared by the authors, (2024).

2.1. Data Acquisition

To characterize the physical environment (geology, geomorphology, pedology, hydrography, and vegetation), cartographic data from the Brazilian Institute of Geography and Statistics (IBGE) at a 1:250,000 scale were used. These resources are accessible online at <https://www.ibge.gov.br/geociencias/downloads-geociencias.html>.

Given the absence of meteorological stations near the study area, data from the Climate Hazards group Infrared Precipitation with Stations (CHIRPS) sensor, proposed by Funk et al. (2015) and applied to Brazil by Costa et al. (2019), were used. These data have a spatial resolution of 0.05° (~ 5 km) and are available at: <https://www.chc.ucsb.edu/data/chirps>, in Esri Bil, GeoTiff and NetCDF formats.

Studies indicate that validation for Brazil is reliable data, therefore plausible for use in different purposes related to climate research, especially in less developed regions or regions with low population density where there is still a shortage of information from meteorological stations, becoming an option for climate studies for tropical and subtropical regions (BAYISSA et al., 2017; PAREDES-TREJO, BARBOSA, and KUMAR, 2017; COSTA et al., 2019).

To constitute the multi-temporal series, four optical images from the Landsat 5 satellite for the years 1992 and 2005 and from Landsat 8 for the years 2014 and 2022 were selected, on the website of the United States Geological Survey (USGS) available at <https://earthexplorer.usgs.gov/> (Table 1).

The criteria for choosing the images were: 1) low cloud cover, 2) high tide to avoid variations in the detection of the position of the coastlines in the tidal flats, this control is done by checking the date and time of image capture combined with data on the tide tables available on the navy website, to verify whether the tide was high or low at the time the image was taken, and finally 3) level 2 (L2) images. The Landsat Level L2 dataset is the standard product of TOA reflectance, therefore, no additional preprocessing is necessary as they present acceptable levels of radiometric calibration and orthorectification (ROY et al., 2014; DWYER et al., 2018).

Table 1. Raster and Vector Database.

IMAGES LANDSAT						
Sensor	orbit point	Scene period	Special Resolution	NDWI/Bands	Climatic Conditions	Tide conditions
TM	225/059	13/06/1992	30m	4,2	Beginning of the drought	High tide
		19/07/2005				
OLI	225/059	13/08/2014	30m	5,3	drought	High tide
		12/09/2022				

The fieldwork includes three trips carried out in the periods (02/09/2021, 06/10/2022 and 25/05/2023) totaling 20 monitored communities: Itamatatuba, Ilhinha, Foz do Gurijuba, Junco, Andiroba, São Pedro, Carneiro, Buritizal, Jaranduba, Vila Progresso, Macedônia, Marinheiro, Franco Grande, Franquinho, Boa Esperança, Arraiol, Livramento, Maranata, Equador and Filadélfia. In these communities, 40cm aluminum markers were installed to measure the distance from the marker to the shore, and a drone flight was also carried out, model Mavic Mini 2 from DJI.

2.2. Shoreline Data Processing

Data processing was conducted using QGIS 3.10.1. The steps included calculating the Normalized Difference Water Index (NDWI) to distinguish land from water, binarization, vectorization, noise removal, smoothing, and final corrections (Figure 3).

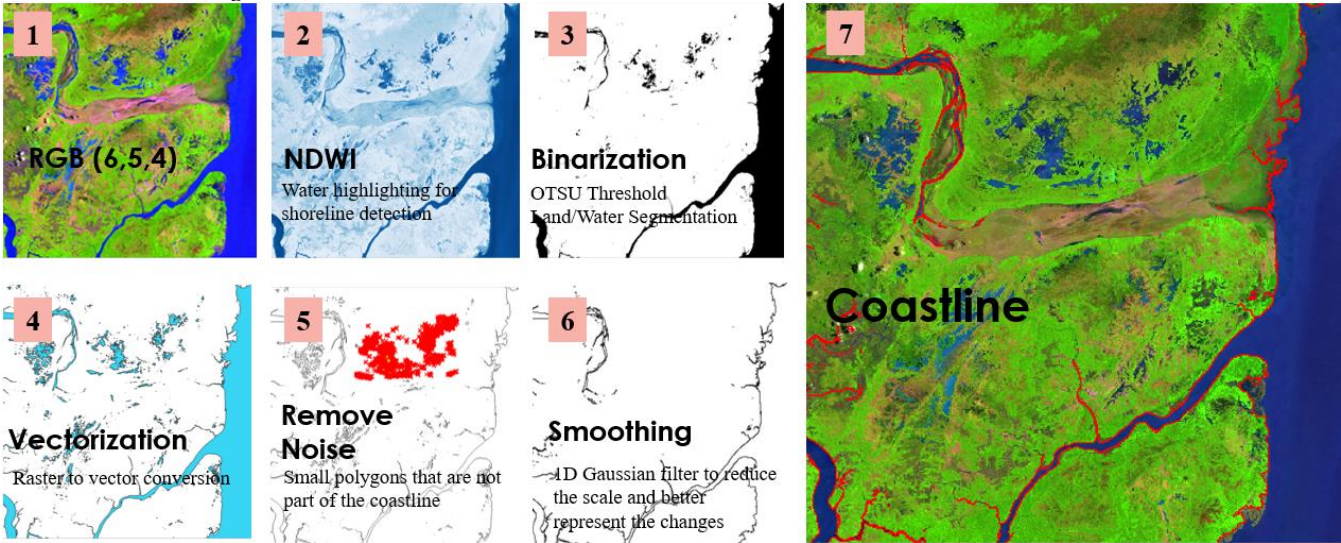


Figure 3. Coastline Extraction Stages. Source: Prepared by the authors, (2024).

The NDWI index is derived from the near-infrared (NIR) and green bands. It is used to enhance water in multispectral images, facilitating the distinction between land and seawater (MCFEETERS, 1996). Bands 2 and 4 of Landsat-5, and bands 3 and 5 of Landsat-8 were used, where the TOA reflectance value of the green band and the

NIR band is more suitable in the calculation of NDWI, compared with the raw Digital Numbers (DN), the NDWI can be calculated directly as:

$$NDWI_{Landsat\ 5} = \frac{(band\ 2 - band\ 4)}{(band\ 2 + band\ 4)} \quad NDWI_{Landsat\ 8} = \frac{(band\ 3 - band\ 5)}{(band\ 3 + band\ 5)}$$

Thresholding is the method of merging NDWI and image binarization. It is a conceptually simple technique that uses a histogram to segment images. In this study, the threshold segmentation method was used (OTSU, 1975). Recent studies have been using this technique to map changes in coastal areas from Landsat images in temporal analysis (KULELI et al., 2011; LUIJENDIJK et al., 2018; ZHOU et al., 2023). In QGIS 3.10.1, this process is done through the Plugin Binarization Threshold plugin.

In this plugin, numerous tests were performed, and to help identify the transition, the line of adult mangrove vegetation was used as a geoindicator, which remains invariable regardless of the tidal conditions, considering that mangrove vegetation constitutes one of the best environments for spatial analysis of coastal environments from orbital remote sensors (SOUZA FILHO and PARADELLA, 2003; FROMARD et al., 2004; CHU et al., 2006; SOUZA FILHO, MARTINS and COSTA, 2006). The thresholds that presented results closest to the transition between dry and wet areas are shown in Table 1.

Table 1. Threshold Values Adopted for Edge Detection.

SENSOR	LANDSAT 5			LANDSAT 8	
	1985	1992	2005	2014	2022
THRESHOLD	Upper: 1,0000	Upper: 1,0000	Upper: 1,0000	Upper: 1,0000	Upper: 1,0000
VALUE	Lower: -0.1764	Lower: -0,1652	Lower: -0,1666	Lower: -0.1009	Lower: -0,0551

Prepared by the authors, (2024).

A 1D Gaussian filter was used for smoothing due to the need to reduce the scale and better visualize the changes, given the spatial resolution of the sensor (MCMASTER and SHEA, 1992). The quantification of the changes was done using the change polygon method, which represents an alternation of regions that are undergoing the erosion or accretion process, providing values for the displacements of the coastal segments (SMITH and CROMLEY, 2012; ALBUQUERQUE et al., 2013).

However, to calculate the average annual erosion rate in the communities, and aiming to obtain information on a more representative scale, a 200-meter buffer was adopted as a reference. This proposal was necessary due to the great variation in the extension of the communities, ensuring that all of them have a uniform sampling.

3. Results

3.1. Analysis of Erosive and Accretionary Dynamics between 1992 and 2022

Between 1992 and 2005 (13 years), approximately 53% of the areas were subjected to accretion, totaling 82.39 km², with an average annual advance rate of 6.4 km². Erosion affected 47% of the areas, corresponding to approximately 72.73 km², with an average annual retreat rate of 5.6 km². Between 2005 and 2014 (9 years), approximately 55% of the areas were subjected to accretion, totaling 134.35 km², with an average annual advance rate of 14.9 km². Erosion reached 45%, equivalent to 111.87 km², with an average annual retreat rate of 12.4 km².

Between 2014 and 2022 (8 years), approximately 60% of the areas were subjected to accretion, totaling 175.82 km², with an average annual advance rate of 21.9 km². Erosion reached 40%, approximately 117.23 km², with an average annual retreat rate of 14.6 km². Between 1992 and 2022 (30 years), approximately 60% of the areas were subjected to accretion, totaling 277.47 km², with an average annual advance rate of 9.08 km². Erosion reached 40%, equivalent to 181.77 km², and an average annual retreat rate of 6.06 km².

It was possible to observe that, over these thirty years, accretion processes predominated in all intervals, with emphasis on the period between 2005 and 2014, when the mouth of the Araguari River was filled and a new configuration of local hydrodynamics occurred (Figure 4).

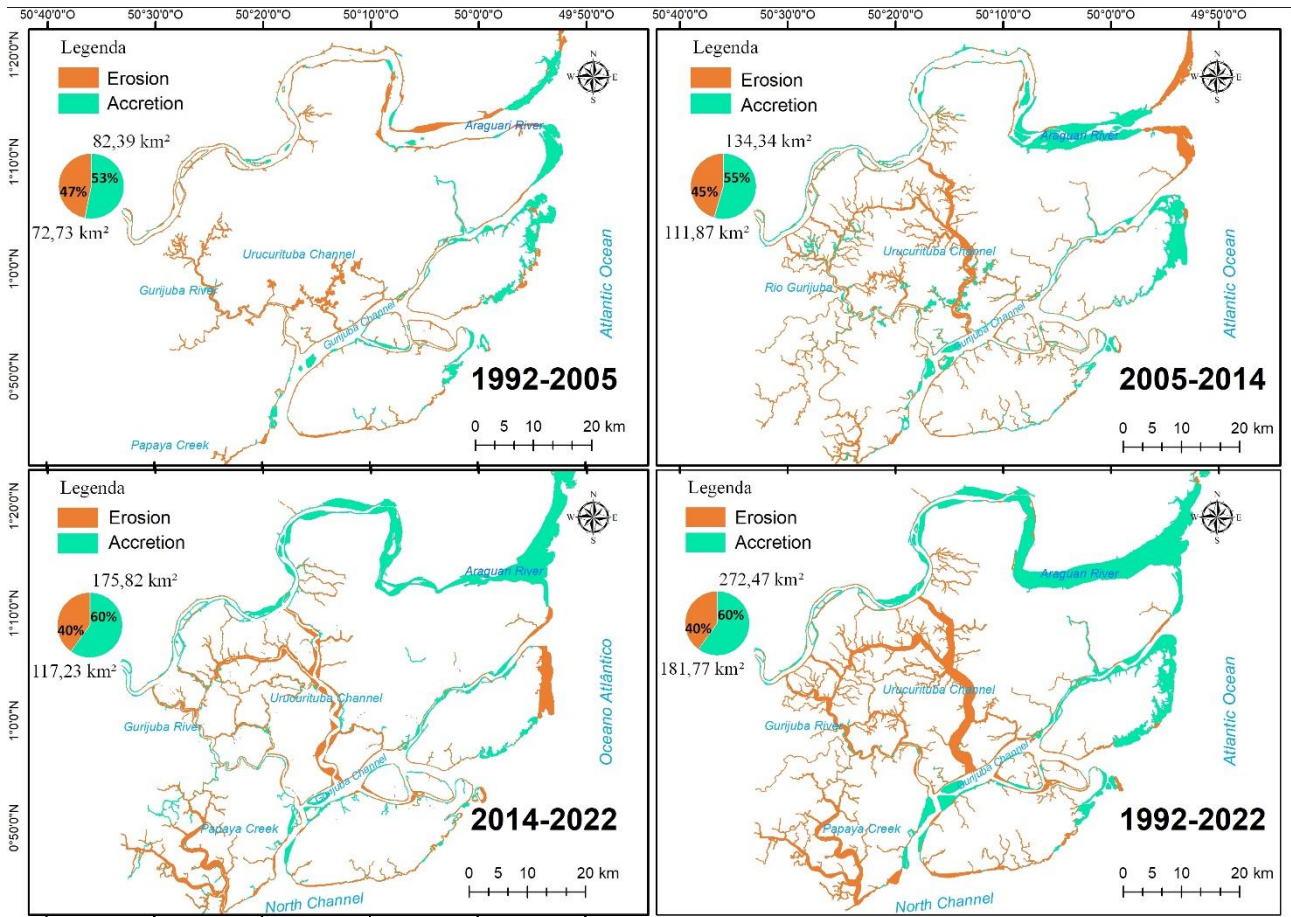


Figure 4. Coastline Change Rates between 1992 and 2022. Prepared by the authors, (2024)

An analysis based on the spatialization of the Erosive and Accretionary Dynamics integrated with the vegetation patterns allowed the delimitation of three zones: 1) Zones with Predominance of Accretion Processes (ZPPA), 2) Mixed Zones with Erosion and Accretion Processes (ZMPEA) and 3) Zones with Predominance of Erosive Processes (ZPPE) (Figure 5).

These zones reflect the main changes in the area over the last thirty years, due to the sedimentary dynamics, the new hydrodynamic configuration, the process of clogging of the mouth of the Araguari River, considering the physiographic characteristics on a local scale. However, it is worth noting that the trends proposed in these zones will only solidify if the current conditions remain, and there may be changes, considering that the region is always changing.

However, it may support government actions for infrastructure projects, community relocation and risk management policies considering the highly limiting fragility of the area, the scale, the data analyzed and the fact that it is the only most up-to-date proposal on the subject in the region.

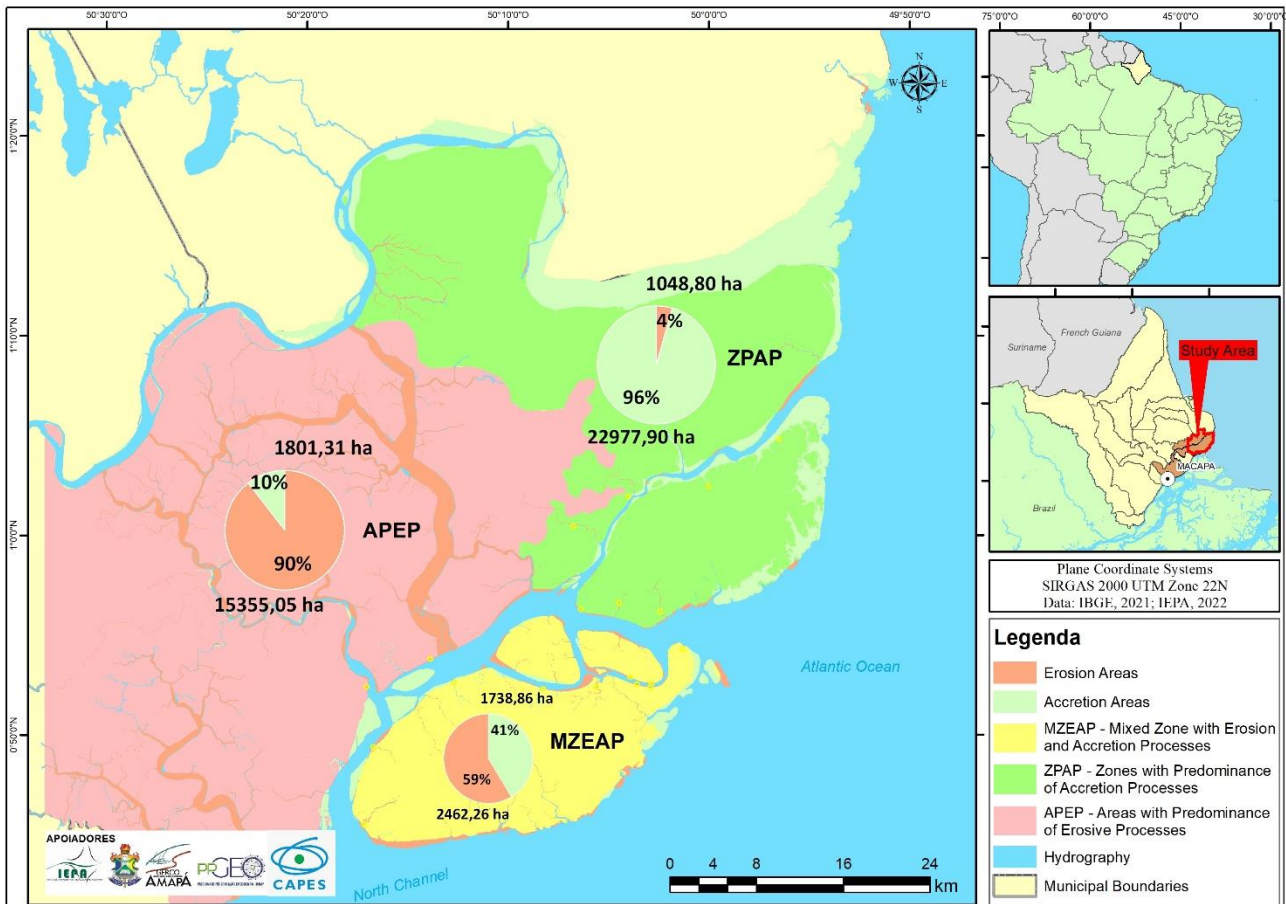


Figure 5. Map showing accretion and erosion zones. Prepared by the authors, (2024)

3.1.1. Zones with Predominance of Accretion Processes (ZPAP)

In this zone, accretion processes reached 96%, equivalent to 22,970 hectares. Clogging processes, formation of tidal flats and headland and central bars are observed. Pioneer and alluvial formations predominate, which are under pressure from intense buffalo farming activities on the banks of the Araguari River and the Igarapé Terra Grande.

The main highlight is the clogging process at the mouth of the Araguari River, characterized by the formation of recent sedimentary deposits, represented by headland bars, mid-channel bars, intertidal and flood plains. These formations result from the forces acting on this estuary (COSTA, 1996).

Calculations performed in this section of the river mouth over the 30 years showed that accretion reached approximately 99%, equivalent to 16,791.90 ha, with an average annual rate of 559.73 ha. Erosion, which was 1%, corresponded to 157.83 ha, with an average annual retreat rate of 5.26 ha (Figure 6).

For Silveira (1998), this process is common in the estuaries of the Amapá coast. However, in this portion, the river is at a lower level than the Southern belt, whose speeds and flow capacities are reduced, facilitating the deposition of sediments close to the mouth, influenced by the strong combination of marine and river sediment discharge, in addition to the action of tidal currents and the Amazon River.

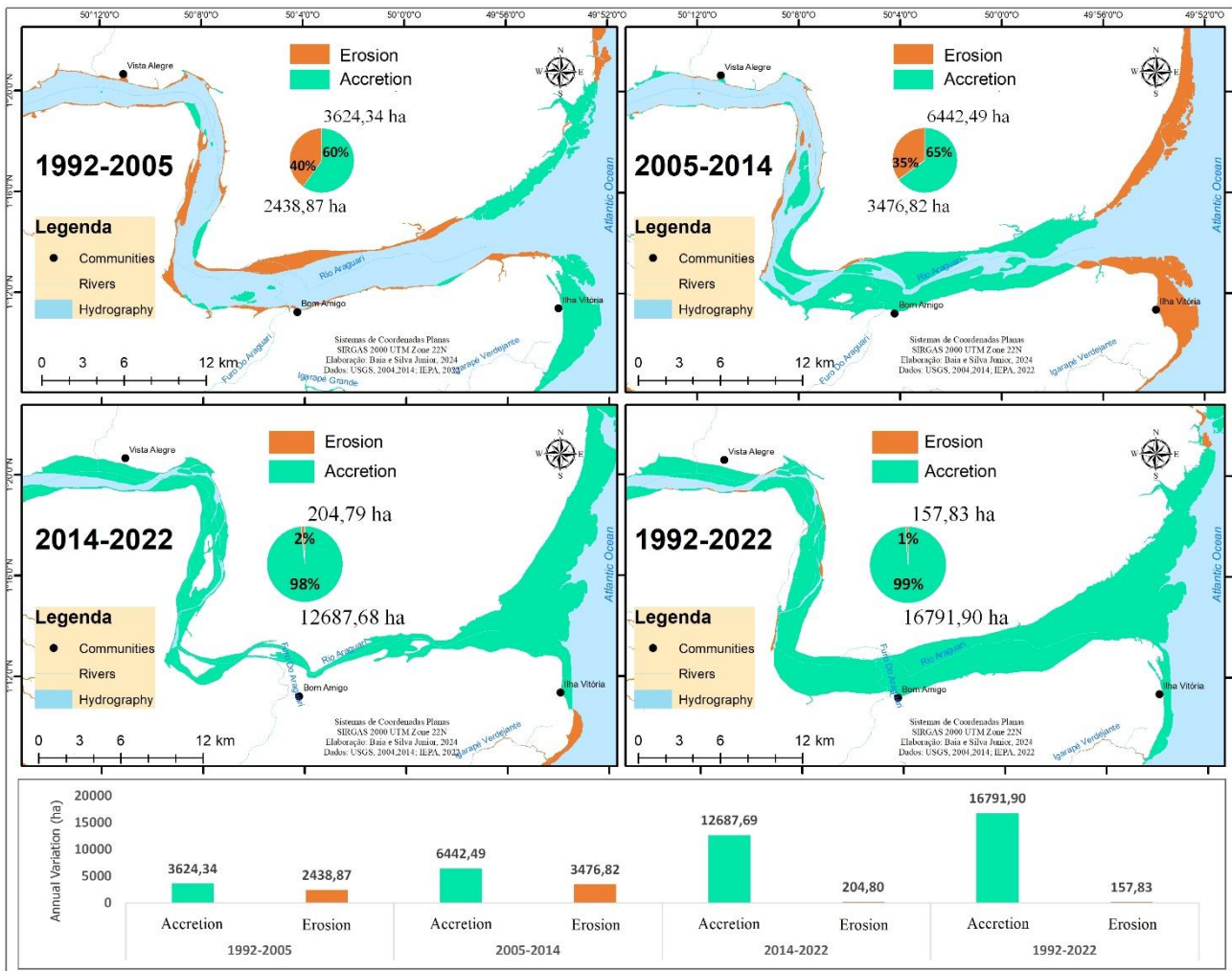


Figure 6. Clogging Process of the Mouth of the Araguari River between 1992 and 2022. Prepared by the authors, (2024)

In this region of Antiga Foz of the Araguari River, numerous farms were installed, triggering a complete change in the ecosystem. The Federal Public Prosecutor's Office requested the State Secretariat for the Environment (SEMA) to adopt appropriate administrative and/or judicial measures to stop the state of degradation. Figure 7 shows images captured during the inspection carried out on May 3, 2023, by SEMA in partnership with the Chico Mendes Institute for Biodiversity Conservation (ICMBio), which suggest an advanced process of ecological succession of pioneer vegetation.



Figure 7. Ecological Succession of Pioneer Vegetation in the Filled Region of the Araguari River Estuary. Caption: (A) Pioneer Vegetation with Fluvial and/or Lacustrine Influence; (B) Farm Fencing; (C) Section of the Old Mouth of the Araguari River. Source: Souza, 2023.

On the Franco and Bailique Islands, the extensive tidal flats along the Gurijuba channel, which separates these islands from the mainland, stand out, in addition to the formations of point bars in the area of contact with the ocean. Calculations show that the accretion rate is approximately 96%, equivalent to 4502.48 ha, with an average annual rate of 150.08 ha. Erosion reached 192.56 ha, equivalent to 4%, and an average annual retreat rate of 6.42 ha (Figure 8).

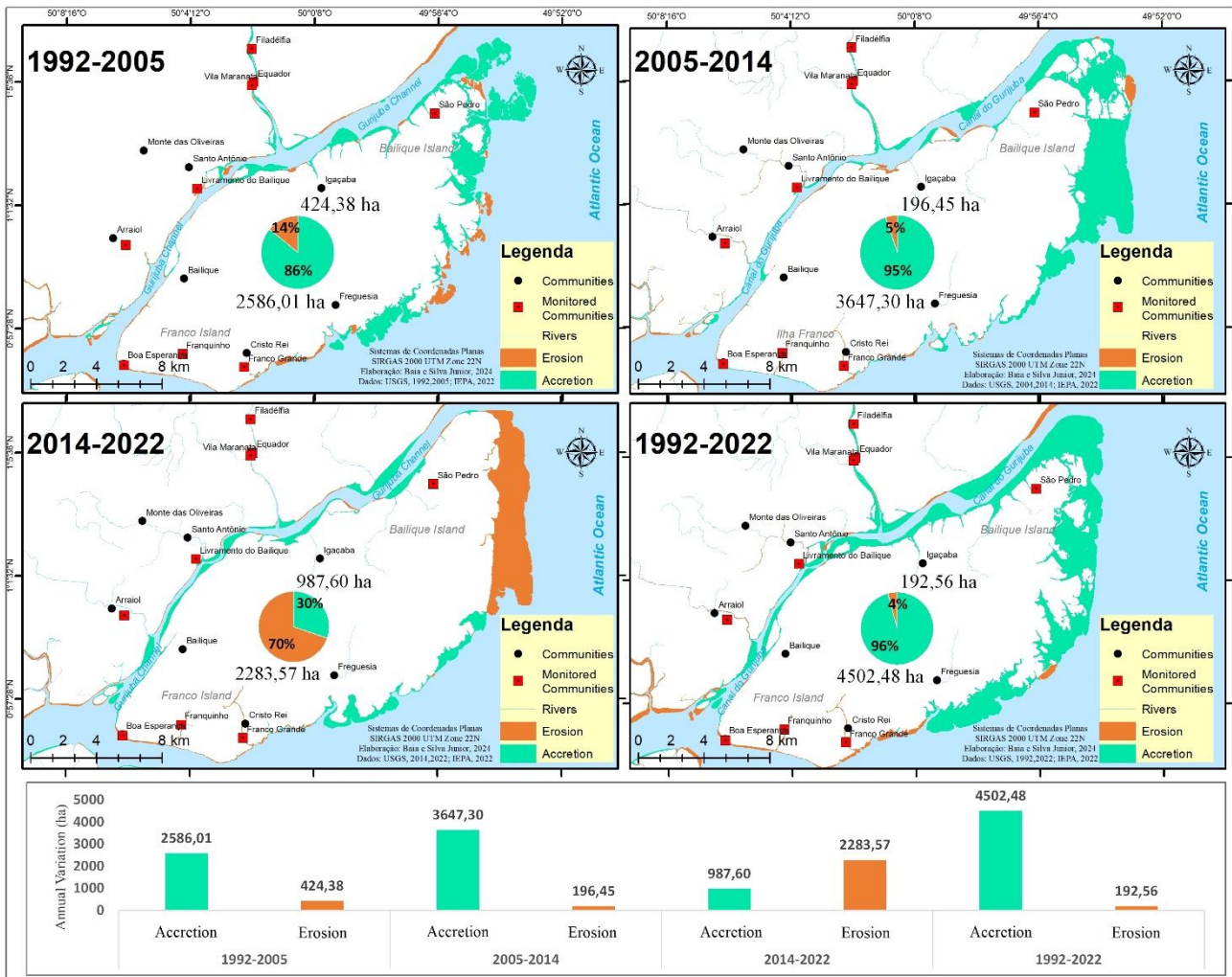


Figure 8. Barra Formation Process in Pontais on the Franco and Bailique Islands between 1992 and 2022. Prepared by the authors, (2024)

If current conditions continue, the islands of Franco and Bailique will probably connect to the mainland. This hypothesis is supported by the accelerated silting caused by the formation of tidal flats and the succession of vegetation, which is reducing the channel bed and making access to the communities of Arraiol, Eluzay, Livramento, Maranhata, Equador and São Pedro more difficult (Figure 9).

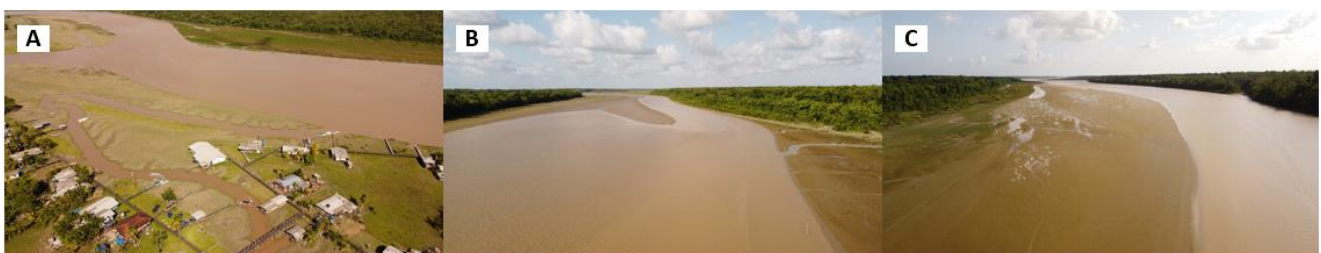


Figure 9. Tidal flats in the process of vegetation succession. Caption: (A) Livramento Community; (B and C) Tidal flat in the Gurijuba Channel. Source: field data, 2022.

3.1.2. Mixed Zone with Erosion and Accretion Processes (MZEAP)

In this zone, erosion and accretion processes occur simultaneously with a small difference in variation. The accretionary areas reached approximately 41%, equivalent to 17.38 thousand hectares, and erosion reached 59%, equivalent to 24.62 thousand hectares (Figure 10). It is characterized by the predominance of muddy bank features, tidal flats, pioneer formations with fluvial-marine influence and alluvial formations, and also concentrates a larger population and commercial activity. Between 1992 and 2022, Curuá and Marinheiro totaled 1,134.29 ha of accretion areas, approximately 53% with an annual rate of 37.81 ha, erosion 1,011.80 ha equivalent to 47% and an annual retreat rate of 33.73 ha. Faustino Island reached 153.17 ha of accretion, approximately 50%, an annual rate of 5.11 ha, erosion 152.94 ha equivalent to 50% and an average annual rate of 5.10 ha.

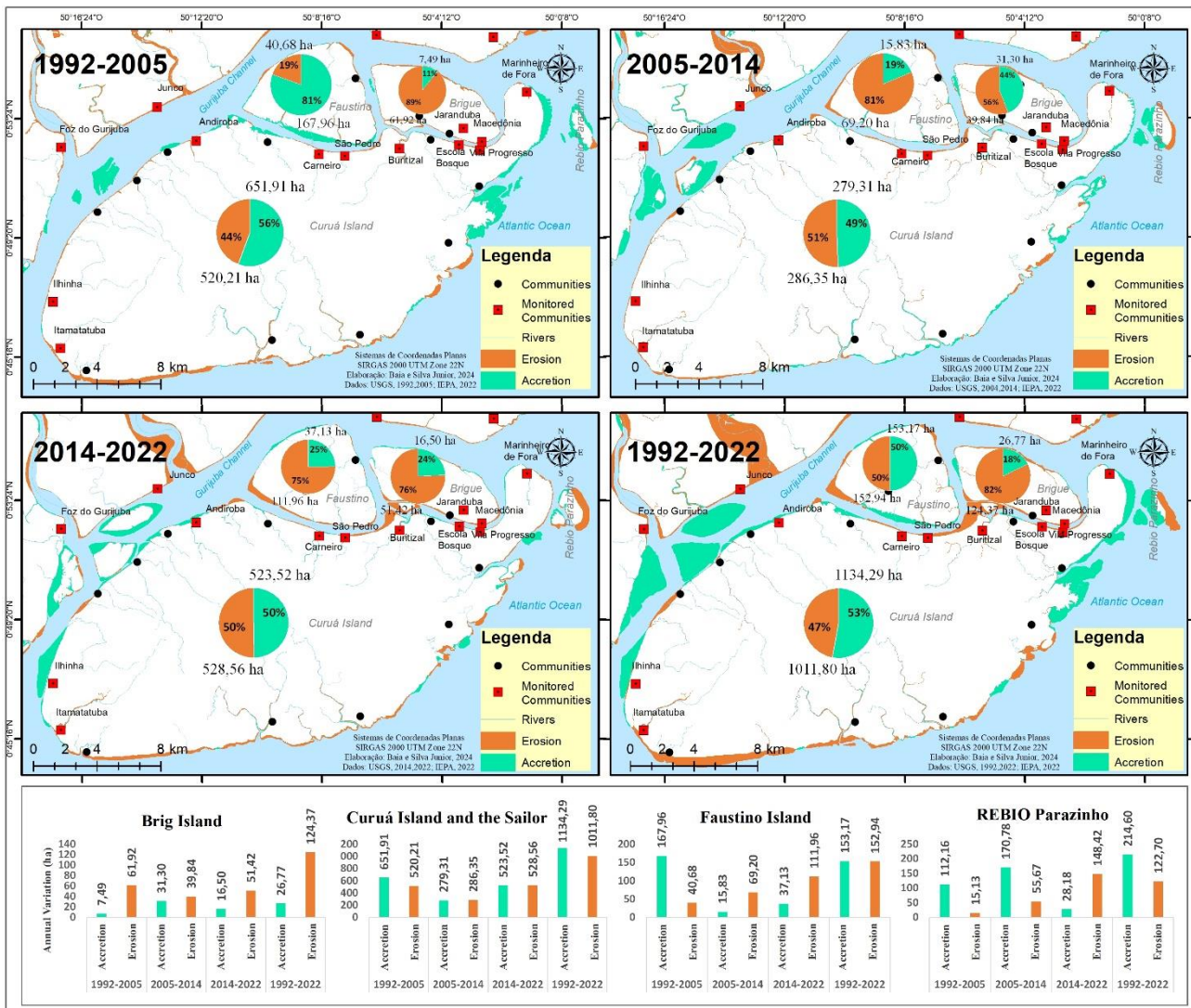


Figure 10. Accretion and erosion process on the islands of Curuá, Brigue and Faustino between 1992 and 2022. Prepared by the authors, (2024)

During this same period, Brigue Island had a total of 26.77 ha of accretion areas, approximately 18%, an annual rate of 0.89 ha; erosion reached 124.37 ha, approximately 82%, an annual retreat rate of 4.15 ha. REBIO Parazinho had a total of 214.60 ha of accretion areas, approximately 64%, with an annual rate of 7.15 ha; erosion reached 122.70 ha, equivalent to 36%, and an average annual rate of 4.09 ha.

One of the factors that reflect the small variation between the erosion and accretion rates is the large contribution of sediments and nutrients received from the Amazon River and the Araguari River, dynamizing the Gurijuba channel, which are responsible for the formation of muddy banks, colonization and growth of pioneer

vegetation (Figure 11). Salinity and tidal regime are decisive in the selection of plant species, in addition, the dynamics of erosion and sediment deposition create favorable conditions for establishment (RAHMAN, 2020).



Figure 11. Muddy Banks with Consolidated Vegetation Succession Process. Caption: (A) Jaburuzinho Community, (B) Junco Community and (C) Boca Velha Beach.

3.1.3. Areas with Predominance of Erosive Processes (APEP)

In this area, erosion processes have reached approximately 90%, equivalent to 15,350 hectares. The opening and widening of drainages prevails, with emphasis on the capture of the flow of water from the Araguari River by the Gurijuba River and the Uricurituba Canal, which previously flowed into the ocean and passed on to the Amazon River. The predominant vegetation cover is floodplains where buffalo farming is carried out.

Between 1992 and 2022, the Gurijuba River totaled 1,533.54 ha of eroded areas (without considering tributaries), approximately 95% with an annual rate of 51.12 ha, an increase of 81.91 ha, equivalent to 5%, and an annual advance rate of 2.73 ha. The Uricurituba totaled 4946.87 ha of eroded areas (not counting tributaries) approximately 100%, at an average annual rate of 164.90 ha, an increase of 4.52 ha equivalent to an annual advance rate of 0.15 ha (Figure 12).

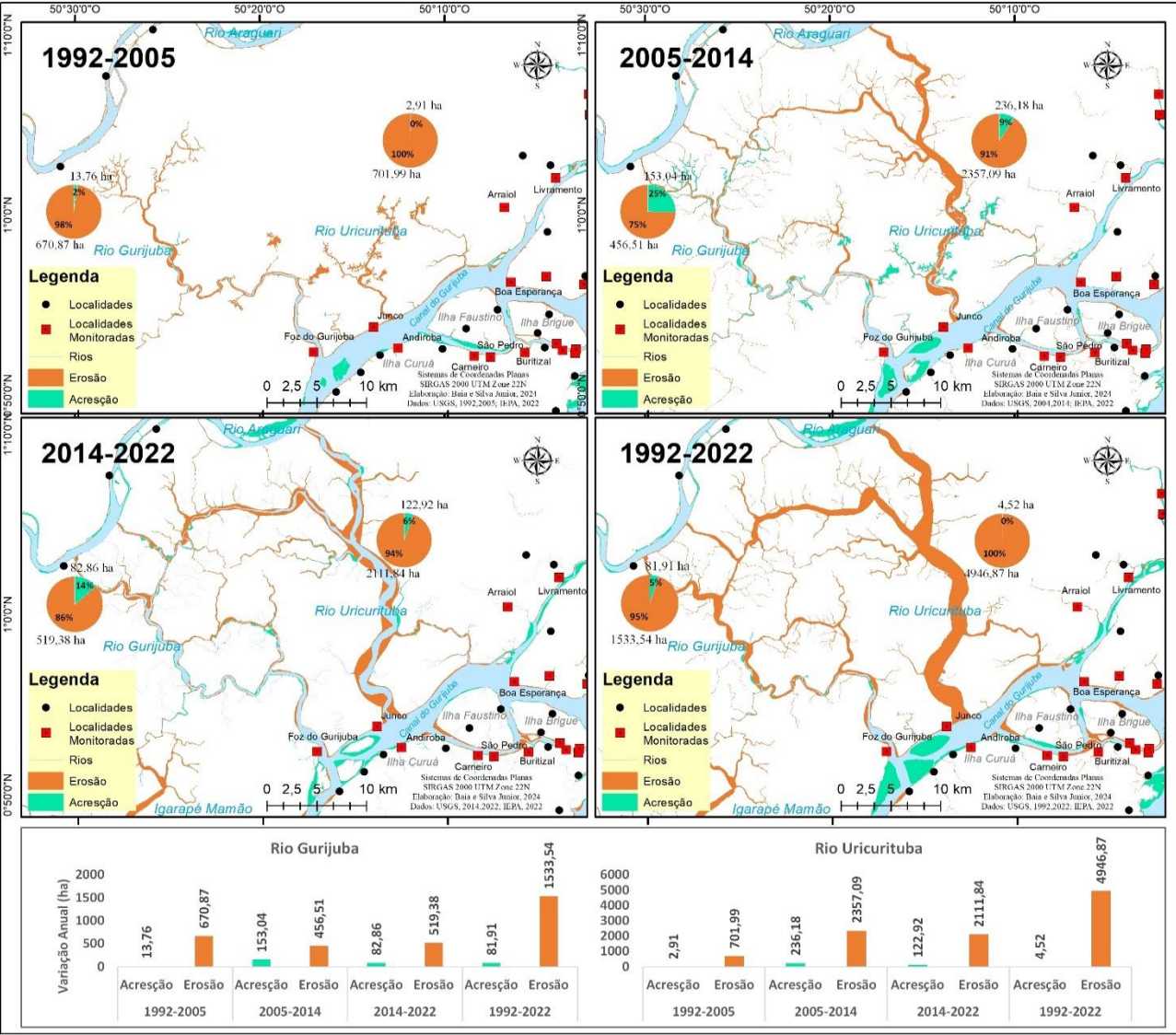


Figure 12. Opening and interconnection of the Araguari, Gurijuba, and Uricurituba rivers between 1992 and 2022.

In 2011, the capture of the Araguari River flow reached approximately 98%, with an average monthly flow ranging from 190 m³/s (November) to 1916 m³/s (March) (SANTOS et al., 2018) (Figure 13). The increase in flow speed due to the new hydrodynamic configuration is responsible for changes such as changes in the sediment balance, flow intensity and currents in the archipelago. The Uricurituba was a small channel used to water animals, and is currently the largest in this portion. The communities of Junco and Foz do Gurijuba are also located here, both with the highest rates of erosion processes, ranking first and second, respectively.

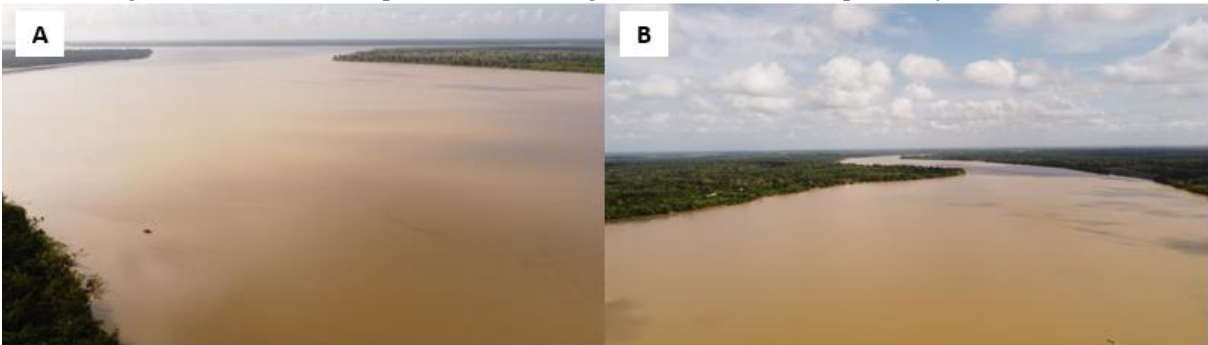
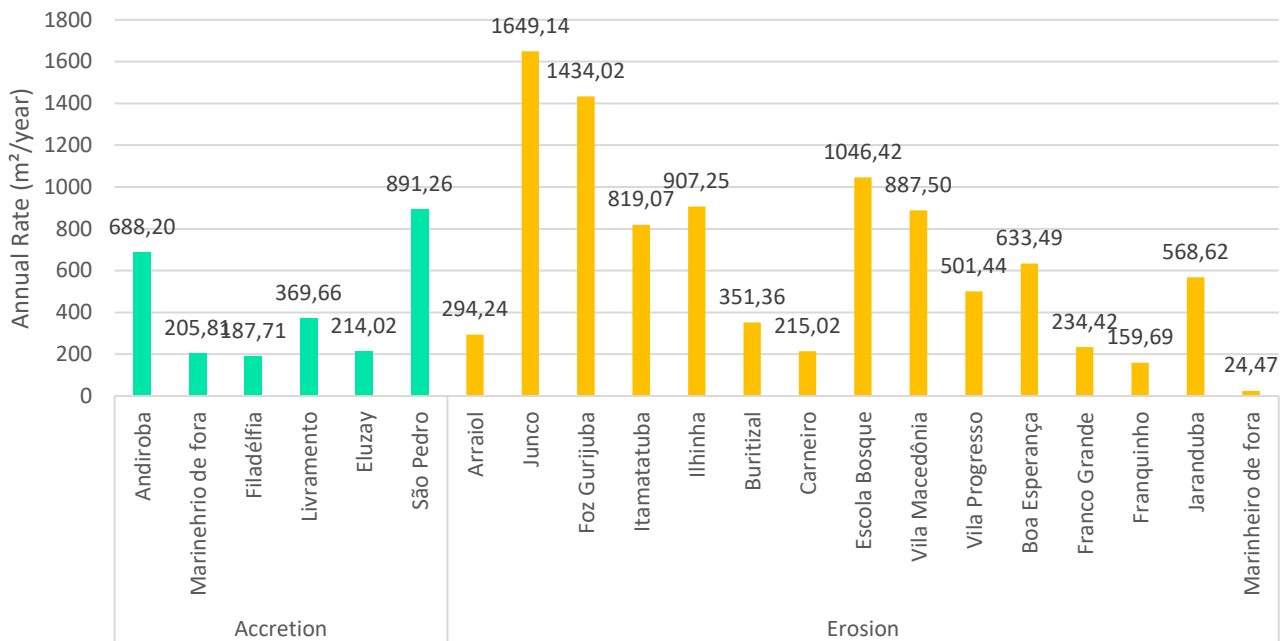


Figure 13. Mouths of the Gurijuba and Uricurituba Rivers. Caption: (A) Mouth of the Uricurituba River and (B) mouth of the Gurijuba River. Source: field data, 2022.

3.1. Impactos nas Comunidades Locais

The impacts on communities are associated with erosion processes. Of the 20 communities monitored, 15 are suffering from erosion, which has caused the loss of homes, schools, businesses and lack of electricity. More recently, with the new configuration of local hydrodynamics, saline intrusion has intensified, and consequently the scarcity of drinking water. Among the communities most affected by erosion are Junco, Foz do Gurijuba, Escola Bosque, Ilhinha, Macedônia, Itamatatuba, Boa Esperança and Vila Progresso (Graph 2).



Graph 2. Average Annual Rate of Erosion and Accretion in Communities between 1992 and 2022.

In this study, the stretch of the Bosque School and the Ilhinha community, both located on Curuá Island (Figure 14), deserve to be highlighted. The stretch of the school is approximately 1 km long and has the third highest erosion rate, with an estimated average annual rate of 1,046.4 m²/year and a linear rate of 10.2 m/year. Opened in 2011, the school was set back approximately fifty meters from the shore. In 2022, the last block was compromised. The government is studying a suitable location for the construction of the new school.

In turn, the Ilhinha community is 0.5 km long and has the fourth highest rate of erosion processes, with an estimated erosion rate of 819.0 m²/year. The linear erosion rate at this point is estimated at 6.4 m/year. In this location in 2017 the bridge that crosses the community was 27 meters from the bank, however, in 2022 it was reduced to around 3 meters, as a result of which many houses are being built on the banks of the nearby stream.



Figure 14. Structure of the Bosque School and Itamatatuba Community.

The communities of Macedônia and Progresso are located on the islands of Brigue and Curuá, respectively (Figure 15). Macedônia is approximately 1.6 km long and has the fifth highest erosion rate, reaching an average annual rate of 887.5 m²/year and a linear rate of 10.55 m/year. Vila Progresso is approximately 1.5 km long and has the eighth highest erosion rate, reaching an average annual rate of 501.4 m²/year and a linear rate of 10.2 m/year. Both are the most influential in the archipelago in terms of size, population and local economy.



Figure 15. Community of Vila Progresso and Macedônia.

The communities of Itamatatuba and Boa Esperança are located on the islands of Curuá and Brigue, respectively (Figure 16). Itamatatuba is approximately 0.5 km long and has the sixth highest erosion rate, an estimated rate of 819.0 m²/year, and an estimated linear erosion rate of 5.25 m/year. In 2017, the structure of the school, health center and ice factory were set back approximately 2 to 4 meters from the shore; in 2022, they were also washed away by erosion.

Boa Esperança, on the other hand, is 0.4 km long and is in seventh place with the highest rates of erosion processes, with an average annual rate of 633.49 m²/year and an estimated linear rate at this point of 2.4 m/year. At this location, the structure of the old school was washed away by the waters in a period of 5 years, with the new buildings being set back from the shore.

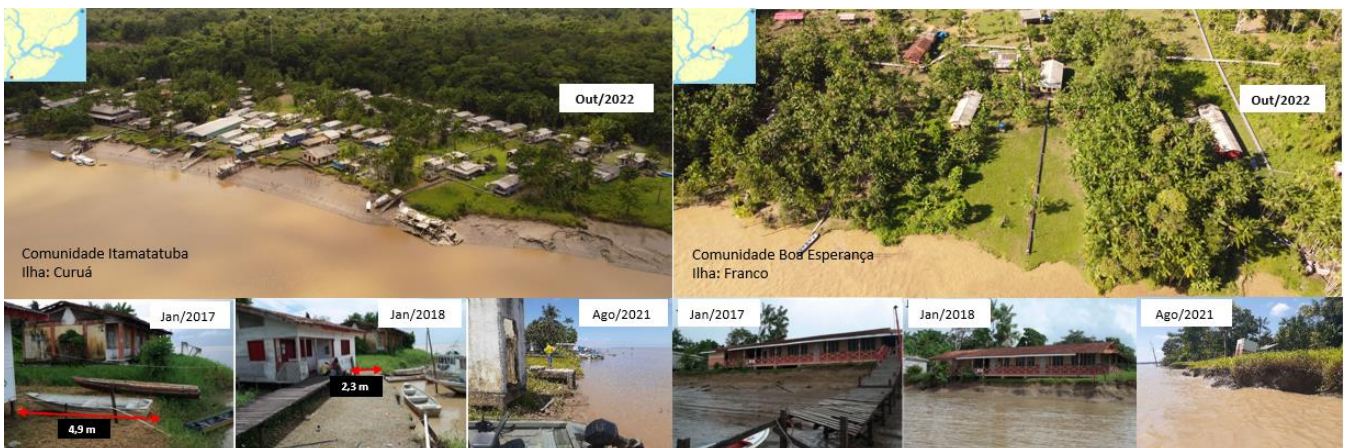


Figure 16. Community of Itamatatuba and Boa Esperança.

Although the archipelago has been part of the National Interconnected System (SIN) since 2015, the lack of electricity and the scarcity of drinking water are recurring problems, due to the constant ruptures in the electrical grid due to fallen poles, which has led local residents to use a hybrid system (energy from the concessionaire, photovoltaic, diesel system). This integration has helped supply local businesses for food preservation (Figure 17a, b, c).

During the dry season, with the new configuration of local hydrodynamics, saline intrusion has intensified, and consequently the scarcity of drinking water. Surface measurements identified the highest salinity levels in the communities of Filadélfia, Maranata, and Equador, located further inland, directed by the current coming from the Atlantic Ocean (SILVA JUNIOR, SZLAFSZTEIN and BAIA, 2022). In response, the assistance measures adopted by the state government have focused on the distribution of mineral water, basic food baskets and water tanks for rainwater collection, storage and primary treatment (Figure 17d, e).



Figure 17. Energy Distribution and Water Collection System. Caption: (A) Electric Pole being carried away by erosion; (B) Photovoltaic Energy System; (C) Diesel Electric System; (D) Rainwater Collection System, Maranata Community; (E) Desalination Plant, Franquinho Community. Source: field data, 2022.

It is worth noting that in estuaries, saline intrusion causes changes in water density, increased turbulence, and changes in sediment circulation and mangrove distribution. These combined effects can lead to increased erosion and habitat loss, especially in mangrove areas, which play a fundamental role in coastal protection, reproduction, feeding, development and refuge for species (CAPO et al., 2006; DANIAL et al., 2021).

4. Discussion

Short-term morphological changes in coastal and estuarine environments are associated with the integrated action of natural agents and anthropogenic factors. These processes and modifications are exacerbated by climate variations and have been widely studied in several regions of the world.

Jolivet et al. (2018) identified, through geospatial analyses and historical data, that the interaction between the sediments of the Amazon River and regional ocean currents contributes to high variability in the position of the coastline on time scales ranging from decades to months on the northern coast of South America. For Talke and Jay (2020), human activities play an important role in increasing tidal amplitude and flooding patterns in some estuaries, exacerbating the risk of flooding and changes in local hydrodynamics.

Zhang et al. (2022) examining the interactions between natural processes (water flow, sedimentation, and sea level rise) and human interventions (dam construction, dredging, and urbanization) in the Yangtze and Mississippi River deltas identified similarities in wetland loss and coastal erosion largely due to reduced sediment transported by rivers due to upstream human activities.

On the Amazon Coast and in the Amapá Coastal Zone, the high dynamism of the region is attributed to pressures from local agents (atmospheric, oceanographic and Amazonian hydrography in the form of water discharge, solid and sediment plumes) and global agents such as climate change, which causes great morphological instability, responsible for changes in the configuration of coastal environments and coastal ecosystems, and consequently in the evolution of this area on a small time scale (BATISTA et al., 2009; SILVA JUNIOR et al., 2021).

The action of atmospheric agents influences the great variation in the precipitation and flooding regime, especially the ITCZ, a band where the northeast trade winds meet the southeast. These winds change direction throughout the year, blowing from the east between October and December, and from the northeast, between January and March. During the dry season, there is a reduction in the flow and discharge of rivers, facilitating the entry of the saline wedge along the estuary, and during the rainy season there is greater soil saturation and an increase in the flow of rivers, intensifying erosion (SALATI and MARQUES, 1981; LENTZ, 1995; VAREJÃO-SILVA, 2006; VALLE-LEVINSON, 2017; FASSONI-ANDRADE et al., 2022).

Oceanographic agents act through the circulation of waves, currents, the macrotidal regime with variable amplitudes that decrease towards the Guiana Coast and the difference in the physical and chemical properties of the water. Because it is a shallow water coast, waves undergo changes in direction such as reflection, refraction and diffraction, conditioning the energy flow (magnitude and direction) resulting in the establishment of coastal circulation patterns, reworking and redistributing unconsolidated sediments perpendicularly or longitudinally along the coastline, causing the loss of wave energy and morphological changes in the beachline (SILVEIRA and SANTOS, 2006; SANTOS, MENDES and SILVEIRA, 2016; SANTOS et al., 2021; SILVA; SILVA JUNIOR; BAIA, 2022).

The Amazonian forcing acts in the form of water, solid and sediment plume discharge. Water discharge refers to the average annual flow of approximately 209,000 m³/s, which corresponds to 18% of the total continental freshwater discharged into the oceans, with maximum values in May (220,000 m³/s) and minimum values in November (100,000 m³/s). Solid discharge is responsible for the high content of suspended material, being highest in February/March and lowest in October/November, with an estimated supply of 1.2 x 10⁹ tons/year (MEADE et al., 1985; MULLER-KARGER et al., 1988; NITTROUER et al., 1995; RANIERI and EL-ROBRINI, 2016).

In turn, the sediment plume is influenced by the high water and sediment discharge (dissolved and particulate) which mixes with the saline waters of the Atlantic Ocean, whose length and thickness vary according to seasonality, extending for 150 to 200 km towards the ocean, and can reach between 100-500 km, supplying sediments on the inner continental shelf (NITTROUER et al., 1991; LENTZ and LIMEBURNER, 1995). According to Geyer et al. (1996), the estuarine plume reaches varied speeds, 83 cm/s on the middle continental shelf and 46 cm/s on the inner continental shelf; however, it decreases from 46 cm/s at a depth of 32 m to 11 cm/s at a depth of 62 m (MUEHE, 1995; ALLISON et al., 1995; SANTOS, 2006).

In the study area, Araújo and Rossete (2023), when superimposing use and coverage, observed that the high fragility of the area is impacted by buffalo farming activities and hydroelectric plants. Santos et al. (2018) Silva Junior et al. (2021) highlight that the magnitude of the effects of these activities is due to the physiographic characteristics, linked to the recent nature of the Quaternary deposits, hydromorphic soils with excess moisture and low load-bearing capacity due to the inconsistent substrate, sensitive to cattle trampling.

Bubalo farming is the main economic activity and has generated numerous discussions about changes in the morphology of the terrain, with the formation of trails, ramps, ravines and ditches, altering the vegetation cover and water quality parameters. This argument is solidified when compared to the coast of Pará, where this practice has been developed for longer and with greater expressiveness, however the effects are smaller considering the differences in the lithological characteristics (FRANÇA and SOUZA-FILHO, 2003).

In turn, the dams of the Cachoeira Caldeirão, Ferreira Gomes and Coaracy Nunes Hydroelectric Power Plants installed in the middle course may have influenced the process of clogging the mouth of the Araguari River. Studies carried out on the Nile and Colorado rivers (MILLIMAN and SYVITSKI, 1992; BEST, 2019), Yenisey (BOBROVITSKAYA, ZUBKOVA and MEADE, 1996), Ebro (BATALLA, GOMEZ and KONDALF, 2004), Danube (HUDEK, ŽGANEC and PUSCH, 2020), Yellow and Yangtze (WANG ET AL., 2007; LUO, YANG and ZHANG, 2012; YANG et al., 2017; REN et al., 2021), Mississippi (MEADE, 1996) and Powder (SYVITSKI and KETTNER, 2007) have identified that clogging and erosion processes are more intense in regions where these projects are installed, which develop changes in river flow patterns, loss of sediment transport capacity, changes in the geometry and hydrology of the river, creating imbalances in areas that were previously dynamic and had constant sediment flow.

This article provides a summary of the particularities, characterization of the dynamics and agents responsible for the morphological changes in the lower estuarine coastal sector, mapping the areas with the highest rates of erosion and accretion based on temporal and evolutionary analysis. The environmental impacts on local communities, the activities carried out and the physiographic vulnerability are also discussed, highlighting the

actions already taken by the government with a view to assisting in the selection of the best solutions, with integrated coastal management and engineering works, in the mitigation and adaptation of damages resulting from coastal dynamics.

5. Conclusions

The lack of management of the impacts resulting from processes affecting the coastal zone of Amapá has led to isolated and inappropriate mitigation actions, which has contributed to the worsening of the effects of erosion and the waste of public financial resources. Although the government has acted with social assistance actions, emergency and calamity decrees, little progress has been made in terms of creating specific public policies to address this problem in the study area.

These policies need to be planned with long-term actions, adopting holistic approaches and prevention and adaptation measures, integrating risk management, urban planning, multiple uses of the coastal zone, sustainable development, social and economic inclusion, recognizing the importance of preparing for future challenges in order to protect communities and preserve local biodiversity.

It is worth noting that if current trends continue, including the forecasts of increased extreme weather events and relative sea level rise, more losses of property and land will occur, leading to irreversible changes in morphology, local hydrodynamics, and resulting problems, in an increasingly shorter time frame.

This trend represents the future of facing severe difficulties and conflicts in maintaining local socioeconomic activities and, equally, of populations that continue to move their homes away from the banks or take shelter in creeks without any technical guidance or prior study by the government. This has been triggering new losses and forcing residents to increasingly choose to leave this region, reducing the number of inhabitants over the years.

In order to have good future prospects, it is necessary to create adaptation measures, implement policies, invest in studies for continuous monitoring of processes and activities developed on the coast, and establish indicators for assessing risk and vulnerability of people/goods/ecosystems on a local scale. These studies require the collection of information on sediment balance, bathymetry, currents, waves, winds, tides and sea level rise, which are still scarce, which makes the problem even more serious.

Authors' Contributions: Maxwell Moreira Baia: Maxwell Moreira Baia: Survey, structuring of the geographic database, processing of geographic information, in addition to the adaptation and validation of the proposed methodology for the study area, through geoprocessing and digital cartography, creation of maps and figures, data analysis, software and textual review. Orleno Marques da Silva Junior: Evaluation and structural systematization of the text and comparison of the methodology with others available in the specialized literature, was also responsible for the evaluation of the results and general review of the text and figures.

Acknowledgments: The authors would like to thank the Postgraduate Program in Geography of the Federal University of Amapá (PPGEO/UNIFAP) for logistical support, the Coordination for the Improvement of Higher Education (CAPES) for financial support and the reviewers of RBG for the comments and suggestions that contributed to the final version of the manuscript.

Conflict of Interest: The authors declare that they have no conflict of interest.

Referências

1. ALBUQUERQUE, M.; ESPINOZA, J.; TEIXEIRA, P.; OLIVEIRA, A.; CORRÊA, I.; CALLIARI, L. Erosion or coastal variability: an evaluation of the DSAS and the change polygon methods for the determination of erosive processes on sandy beaches. *Journal of Coastal Research*, v. 65, n. SI, p. 1710-1714, 2013. DOI:0.2112/SI65-289.1
2. ALLISON, M.; NITTROUER, C.; KINEKE, G. Seasonal sediment storage on mudflats adjacent to the Amazon River. *Marine Geology*, v. 125, n. 3-4, p. 303-328, 1995.
3. ANTHONY, E.; BRONDIZIO, E.; SANTOS, V.; GARDEL, A.; BESSET, M. Sustainable Management, Conservation, and Restoration of the Amazon River Delta and Amazon-Influenced Guianas Coast: A Review. *Water*, 13(10), 1371. 2021
4. ARAÚJO, A.; ROSSETE, A. Análise da fragilidade ambiental na bacia hidrográfica do rio Araguari, Amapá-brasil. *REVISTA EQUADOR*, v. 12, n. 3, p. 95-117, 2023. DOI:10.26694/equador.v12i3.13990
5. AUCELLI, P.; MATANO, F.; SALVINI, R.; SCHIATTARELA, M. Editorial – Coastal changes, from past records to future trends: proxy analysis, modelling, and monitoring. *Journal of Coastal Conservation*, 22, 821–825. 2018. doi.org/10.1007/s11852-018-0623-z

6. BATALLA, R.; GOMEZ, C.; KONDOLF, G. Reservoir-induced hydrological changes in the Ebro River basin (NE Spain). **Journal of hydrology**, v. 290, n. 1-2, p. 117-136, 2004. DOI:10.1016/j.jhydrol.2003.12.002
7. BATISTA, E.; SOUZA FILHO, P.; SILVEIRA, O. Avaliação de áreas deposicionais e erosivas em cabos lamosos da zona costeira Amazônica através da análise multitemporal de imagens de sensores remotos. **Revista Brasileira de Geofísica**, [S.l.], v. 27, n. 5, p. 83-96, 2009. DOI:10.1590/S0102-261X2009000500007
8. BAYISSA, Y.; TADESSE, T.; DEMISSE, G.; SHIFERAW, A. Evaluation of Satellite-Based Rainfall Estimates and Application to Monitor Meteorological Drought for the Upper Blue Nile Basin, Ethiopia. *Remote Sensing*, v. 9, n. 7, p. 669, 2017.
9. BEST, J. Anthropogenic stresses on the world's big rivers. **Nature Geoscience**, v. 12, n. 1, p. 7-21, 2019. DOI:10.1038/s41561-018-0262-x
10. BOBROVITSKAYA, N.; ZUBKOVA, C.; MEADE, R. H. Discharges and yields of suspended sediment in the Ob' and Yenisey Rivers of Siberia. **IAHS Publications-Series of Proceedings and Reports-Intern Assoc Hydrological Sciences**, v. 236, p. 115-124, 1996.
11. CAPO, S.; SOTTOLICHIO, A.; BRENON, I.; CASTAING, P.; FERRY, L. Morphology, hydrography and sediment dynamics in a mangrove estuary: the Konkoure Estuary, Guinea. *Marine Geology*, 230(3-4), 199-215, 2006.
12. CHEN, Y.; DUO, L.; ZHAO, D.; ZENG, Y.; GUO, X. The response of ecosystem vulnerability to climate change and human activities in the Poyang lake city group, China. *Environmental Research*, 233, 116473, 2023.
13. COSTA, J.; BEMERGUY, R.; HASUL, Y.; SILVA BORGES, M.; JÚNIOR, C.; BEZERRA, P.; FERNANDES, J. Neotectônica da região amazônica: aspectos tectônicos, geomorfológicos e deposicionais. **Geonomos**, 1996. DOI:10.18285/geonomos.v4i2.199
14. COSTA NETO, S.; SILVA, M. Vegetação. in: santos, v.f. & figueira, z.r. (orgs.). Diagnóstico sócioambiental participativo do setor costeiro estuarino do estado do amapá. Mma/gea/iepa. macapá. meiodigital cd. p. 84-114, 2004.
15. COSTA, J.; PEREIRA, G.; SIQUEIRA, M.; CARDOZO, F.; SILVA, V. Validação dos dados de precipitação estimados pelo CHIRPS para o Brasil. **Revista Brasileira de Climatologia**, v. 24, 2019. DOI:10.5380/abclima.v24i0.60237
16. COSTA, J.; SOUZA, R. Biorecuperação de dunas costeiras do município de Pirambu/SE. In: SOUZA, R. M. (Org.). **Território, planejamento e sustentabilidade: conceitos e práticas**. São Cristóvão: Editora, UFS, 2009.
17. CROSSLAND, C.; KREMER, H.; LINDEBOOM, H.; CROSSLAND, J.; LE TISSIER, M. (EDS.) **Coastal fluxes in the Anthropocene: the land-ocean interactions in the coastal zone project of the International Geosphere-Biosphere Programme**. Springer Science & Business Media, 2005
18. DANIAL K.; WILLIAM G.; VALENTIN H.; STEFAN F. Sea level rise impacts on estuarine dynamics: A review, **Science of The Total Environment**, Volume 780, 146470, ISSN 0048-9697, 2021. <https://doi.org/10.1016/j.scitotenv.2021.146470>.
19. DETHIER, M.; HARPER, J. 1.04-Classes of Nearshore Coasts, Editor(s): Eric Wolanski, Donald McLusky, Treatise on Estuarine and Coastal Science, **Academic Press**, Pages 61-74, ISBN 9780080878850, 2011. DOI:10.1016/B978-0-12-374711-2.00105-4.
20. DWYER, JOHN L.; DAVID P. ROY, BRIAN SAUER, CALLI B. JENKERSON, HANKUI K. ZHANG, AND LEO LYMBURNER. Analysis Ready Data: Enabling Analysis of the Landsat Archive. **Remote Sensing** 10, no. 9: 1363, 2018. DOI:10.3390/rs10091363
21. FASSONI-ANDRADE, A.; PAPA, R.; PAIVA, S. WONGCHUIG, S.; FLEISCHMANN, A. **Amazon Water Cycle Observed from Space**. *Eos*, 2022. 103: p. e2020RG000728. Disponível em: <https://eos.org/editors-vox/amazon-water-cycle-observed-from-space>. Acesso em: 30/10/24.
22. FRANÇA, C.; SOUZA-FILHO, P. M. Análise das mudanças morfológicas costeiras de médio período na margem leste da ilha de marajó (pa) em imagem landsat. **Revista brasileira de geociências**, V. 33, P. 127-136, 2003.
23. HUDEK, H.; ŽGANEC, K.; PUSCH, M. A review of hydropower dams in Southeast Europe—distribution, trends and availability of monitoring data using the example of a multinational Danube catchment subarea. **Renewable and Sustainable Energy Reviews**, v. 117, p. 109434, 2020. DOI:10.1016/j.rser.2019.109434
24. IBGE. Instituto Brasileiro de Geografia e Estatística. Censo 2022: informações de população e domicílios por setores censitários. 2022. Disponível em: <https://agenciadenoticias.ibge.gov.br/agencia-noticias/2012-agencia-de-noticias/noticias/39525-censo-2022-informacoes-de-populacao-e-domicilios-por-setores-censitarios-auxiliam-gestao-publica>.
25. JOLIVET, M.; ANTHONY, E. J.; GARDEL, A.; BRUNIER, G. Multi-decadal to short-term beach and shoreline mobility in a complex river-mouth environment affected by mud from the Amazon. *Frontiers in Earth Science*, v. 7, p. 187, 2019. DOI:10.3389/feart.2019.00187
26. KULELI, T.; GUNEROGLU, A.; KARSLI, F.; DIHKAN, M. Automatic detection of shoreline change on coastal Ramsar wetlands of Turkey. **Ocean Engineering**, v. 38, n. 10, p. 1141-1149, 2011.

27. LENTZ, S. The Amazon River plume during AMASSEDs: subtidal current variability and the importance of wind forcing. **Journal of Geophysical Research: Oceans**, v. 100, n. C2, p. 2377-2390, 1995. DOI:10.1029/94JC00343
28. LENTZ, S.; LIMEBURNER, R. The Amazon River Plume during AMASSEDs: Spatial Characteristics and Salinity Variability. **Journal of Geophysical Research**, 100, 2355-2375. 1995. DOI:10.1029/94JC01411
29. LUIJENDIJK, A.; HAGENAARS, G.; RANASINGHE, R.; BAART, F.; DONCHYTS, G.; AARNINKHOF, S. The state of the world's beaches. **Scientific reports**, v. 8, n. 1, p. 1-11, 2018. DOI:10.1038/s41598-018-24630-6, 2018.
30. LUO, X.; YANG, S.; ZHANG, J. The impact of the Three Gorges Dam on the downstream distribution and texture of sediments along the middle and lower Yangtze River (Changjiang) and its estuary, and subsequent sediment dispersal in the East China Sea. **Geomorphology**, v. 179, p. 126-140, 2012. DOI:10.1016/j.geomorph.2012.05.034
31. MARENGO, J.; SCARANO, F.; KLEIN, A.; SOUZA, C.; CHOU, S. **Impacto, vulnerabilidade e adaptação das cidades costeiras brasileiras às mudanças climáticas**. Relatório Especial do Painel Brasileiro de Mudanças Climáticas (PBMCC), p. 184, 2016.
32. MCMASTER, R.; SHEA, K. **Generalization in digital Cartography**. 1.ed. Washington: Association of American Geographers, 1992.
33. MEADE, R.; DUNNE, T.; RICHEY, J.; SANTOS, U.; SALATI, E. Storage and remobilization of suspended sediment in the lower Amazon River of Brazil. *Science*, v. 228, n. 4698, p. 488-490, 1985.
34. MEADE, R. River-sediment inputs to major deltas. In: **Sea-level rise and coastal subsidence: Causes, consequences, and strategies**. Dordrecht: Springer Netherlands, 1996. p. 63-85.
35. MENTASCHI, L.; VOUSDOKAS, M.; PEKEL, J.; VOUKOUVALAS, E.; FEYEN, L. Global long-term observations of coastal erosion and accretion. **Scientific reports**, 8(1), 1-11, 2018.
36. MILLIMAN J.; SYVITSKI J. Geomorphic/tectonic control of sediment discharge to the ocean: the importance of small mountainous rivers. **The journal of Geology**, v. 100, n. 5, p. 525-544, 1992. DOI:10.1086/629606.
37. MUEHE, D. Geomorfologia Costeira. In: Guerra AJT, Cunha SB (Org.). **Geomorfologia: uma atualização de bases e Conceitos**. 2ª ed., Editora Bertrand Brasil, Rio de Janeiro, p. 253 – 308, 1995.
38. MUEHE D. O litoral brasileiro e sua compartimentação. In: CUNHA SB da & GUERRA AJT. **Geomorfologia do Brasil**. Rio de Janeiro: Bertrand Brasil, 2012.
39. MÜLLER-KARGER, F.; MCCLAIN, C.; FISHER, T.; ESAIAS, W.; VARELA, R. Pigment distribution in the Caribbean Sea: Observations from space. *Progress in Oceanography*, v. 23, n. 1, p. 23-64, 1989. DOI:10.1016/0079-6611(89)90024-4
40. NICHOLLS, R.; WONG, P.; BURKETT, V.; CODIGNOTTO, J.; HAY, J.; MCLEAN, R.; WOODROFFE, C. **Coastal systems and low-lying areas** in: climate change: impacts, adaptation and vulnerability: contribution of working group ii to the fourth assessment report of the intergovernmental panel on climate change, cambridge university press, cambridge, uk, 2007, pp. 315-356.
41. NITTROUER, C.; KUEHL, S.; RINE, J.; FIGUEIREDO, A.; FARIA, L.; DIAS, G.; SILVEIRA, O. Sedimentology and stratigraphy of the Amazon continental shelf. **Oceanography**, v. 4, n. 1, p. 33-38, 1991.
42. NITTROUER, C.; KUEHL, S.; STERNBERG, R.; FIGUEIREDO JR, A.; FARIA, L. An introduction to the geological significance of sediment transport and accumulation on the Amazon continental shelf. **Marine Geology**, v. 125, n. 3-4, p. 177-192, 1995.
43. OTSU, N. A threshold selection method from gray-level histograms. **Automatica**, v. 11, n. 285-296, p. 23-27, 1975.
44. PAREDES-TREJO, F.; BARBOSA, H.; KUMAR, T. Validating CHIRPS-based satellite precipitation estimates in Northeast Brazil. **Journal of arid environments**, v. 139, p. 26-40, 2017.
45. PEREIRA, L.; SILVA, N.; COSTA, R.; ASP, N.; COSTA, K.; VILA-CONCEJO, A. Seasonal changes in oceanographic processes at an equatorial macrotidal beach in northern brazil. **continental shelf research**, v. 43, p. 95–106, 2012.
46. PRESTES, Y.; SILVA, A.; JEANDE, C. Amazon water lenses and the influence of the north brazil current on the continental shelf. **continental shelf research**. v. 160, n. 15, p. 36-48, 2018.
47. RAHMAN, M. Impact of increased salinity on the plant community of the Sundarbans Mangrove of Bangladesh. **Community ecology** 21, 273–284, 2020. DOI:10.1007/s42974-020-00028-1
48. RANIERI, L.; EL-ROBRINI, M. Condição oceanográfica, uso e ocupação da Costa de Salinópolis (Setor Corvina –Atalaia), Nordeste do Pará, Brasil. **Journal of Integrated Coastal Zone Management**, v. 16, n. 2, p. 133–146. 2016. DOI:10.5894/rgci565
49. REN, S.; ZHANG, B.; WANG, W.; YUAN, Y & GUO, C. 2020. Sedimentation and its response to management strategies of the Three Gorges Reservoir, Yangtze River, China, **CATENA**, Volume 199, 105096, ISSN 0341-8162, 2021. DOI:10.1016/j.catena.2020.10509.

50. RODRIGUES, M.; SILVA JUNIOR, O. Panorama Geral da Zona Costeira do Estado do Amapá. **Rev. Bras. De Geogr. Física**, v. 14, p. 1654-1674, 2021. DOI:10.26848/rbgf.v14.3.p1654-1674
51. ROY, D.; WULDER, M.; LOVELAND, T.; WOODCOCK, C.; ALLEN, R.; ANDERSON, M.; ZHU, Z. Landsat-8: Science and product vision for terrestrial global change research. **Remote sensing of Environment**, 145, 154-172, 2014. DOI:10.1016/j.rse.2014.02.001
52. SALATI, E.; MARQUES, J. Climatology of the Amazon region, in *The Amazon: Limnology and Landscape Ecology of a Mighty River and Its Basin*, H. Sioli, Editor. 1981, Dr. W. Junk Publishers: Dordrecht, The Netherlands. p. 85-126.
53. SANTOS, E.; LOPES, P.; PEREIRA, H.; NASCIMENTO, O.; RENNIE, D.; STERNBERG, L.; CUNHA, A. The impact of channel capture on estuarine hydro-morphodynamics and water quality in the Amazon delta. **Science of the Total Environment**. 624 887-899, 2018.
54. SANTOS, V.; MENDES, A.; SILVEIRA, O. Atlas de Sensibilidade Ambiental a derrame de óleo para a bacia marítima da foz do Amazonas. 2016.
55. SANTOS, V. **Ambientes costeiros amazônicos: avaliação de modificações por sensoriamento remoto**. Tese (Doutorado em Ciências), Programa de Pós-Graduação em Geologia e Geofísica Marinha. Universidade Federal Fluminense, Niterói, RJ. 2006. 356p. DOI:10.13140/RG.2.1.5018.4162.
56. SILVA JUNIOR, O.; FUCKNER, M.; BAIA, M.; SILVA, C.; SANTOS, L. Comitê da bacia Hidrográfica do rio Araguari como instrumento de gestão dos Recursos Hídricos no Estado do Amapá. **Revista Brasileira de Geografia Física**, v. 14, n. 05, p. 2771-2789, 2021. DOI:10.26848/rbgf.v14.5.p2771-2789
57. SILVA JUNIOR, O.; SZLAFSZTEIN, C.; BAIA, M. Gestão de riscos de desastres no arquipélago do Bailique, foz do rio Amazonas, Amapá, Brasil. **Ensino de Geografia e Redução de Riscos**. Bauru: AGB, p. 674-696, 2022.
58. SILVA JUNIOR, O.; SANTOS, L.; RODRIGUES, M. Panorama dos Riscos Costeiros no Estado do Amapá: Conhecer para Agir In: **Redução do risco de desastres e a resiliência no meio rural e urbano**. 2 ed. São Paulo: Centro Paula Souza, 2020, v.2, p. 454-472. Disponível em: https://www.agbbauru.org.br/publicacoes/Reducao2020/Reducao_2ed-2020-25.pdf
59. SILVA, M.; SILVA JUNIOR, O.; BAIA, M. Modificações na linha de costa da praia do goiabal (1985-2019) Calçoene-Amapá-Brasil. **Conselho Editorial**, p. 46, 2022.
60. SILVEIRA, O. **A Planície Costeira do Amapá**. Dinâmica de Ambiente Influenciado por Grandes Fontes Fluviais Quaternárias. Tese (Doutorado em Geologia e Geoquímica), Centro de Geociências, Universidade Federal do Pará. Belém. 215p.
61. SILVEIRA, O.; SANTOS, V. Aspectos Geológicos-Geomorfológicos da Região Costeira entre o rio Amapá Grande e a Região dos Lagos do Amapá. In: Salustiano Vilar da Costa Neto. (Org.). **Inventário biológico das Áreas do Sucuriçu e Região dos Lagos no Estado do Amapá**. Macapá: IEPA, 2006, v. unico, p. 17-40.
62. SMITH, M.; CROWLEY, R. Measuring historical coastal change using gis and the change Polygon approach. **Transactions in GIS**, v.16, n.1, p. 3-15, 2012. DOI:10.1111/j.1467-9671.2011.01292.x
63. SOUZA-FILHO, P.; PARADELLA, W. Use of synthetic aperture radar for recognition of Coastal Geomorphological Features, land-use assessment and shoreline changes in Bragança coast, Pará, Northern Brazil. **Anais da Academia Brasileira de Ciências**, 75, 341-356. 2003
64. SOUZA-FILHO, P.; MARTINS, E.; COSTA, F. Using mangroves as a geological indicator of coastal changes in the Bragança macrotidal flat, Brazilian Amazon: a remote sensing data approach. **Ocean & coastal management**, 49(7-8), 462-475. 2006.
65. SOUZA-FILHO, P.; PARADELLA, W.; RODRIGUES, S.; COSTA, F.; MURA, J.; GONÇALVES, F. Discrimination of coastal wetland environments in the amazon region based on multipolarized l-band airborne synthetic aperture radar imagery. **Estuarine, coastal and shelf science**, v. 95, n. 1. 2011. p. 88-98.
66. SYVITSKI, J.; KETTNER, A. On the flux of water and sediment into the Northern Adriatic Sea. **Continental Shelf Research**, v. 27, n. 3-4, p. 296-308, 2007. DOI:10.1016/j.csr.2005.08.029
67. TALKE, S.; JAY, D. Changing tides: The role of natural and anthropogenic factors. **Annual review of marine science**, v. 12, n. 1, p. 121-151, 2020.
68. TORRES, A.; EL-ROBRINI, M.; COSTA, W. Amapá. In: DIETER MUEHE. (ED). **Panorama da erosão costeira no brasil**. 2018. ISBN: 978-85-7738-394-8.
69. VALLE-LEVINSON, A.; DUTTON, A.; & MARTIN, J. B. Spatial and temporal variability of sea level rise hot spots over the eastern United States. **Geophysical Research Letters**, v. 44, n. 15, p. 7876-7882, 2017. doi.org/10.1002/2017GL073926
70. VAREJÃO-SILVA, M. Meteorologia e Climatologia. Versão digital 2. Recife, PB, março, 463p., 2006.
71. VILLWOCK, J.; LESS, G.; SUGUIO, K.; ANGULO, R.; DILLENBURG, S. Geologia e Geomorfologia de Regiões Costeiras. In: SOUZA, C, G; SUGUIO, K.; OLIVEIRA, A, M, S.; OLIVEIRA, P. (ED). **Quaternário do Brasil**. Ribeirão Preto: Holos, Editora, 2005. 382p.

72. WANG H.; YANG Z.; SAITO Y.; LIU J.; SUN X. Stepwise decreases of the Huanghe (Yellow River) sediment load (1950–2005): Impacts of climate change and human activities. **Global and Planetary Change**, v. 57, n. 3–4, p. 331–354, 2007. DOI:10.1016/j.gloplacha.2007.01.003.
73. WATERS, C.; ZALASIEWICZ, J.; SUMMERHAYES, C.; BARNOSKY, A.; POIRIER, C.; GAŁUSZKA, A.; WOLFE, A. The Anthropocene is functionally and stratigraphically distinct from the Holocene. **Science**, v. 351, n. 6269, p. aad2622, 2016. DOI: 10.1126/science.aad2622. PMID: 26744408.
74. YANG, Y.; ZHANG, M.; ZHU, L.; LIU, W.; HAN, J.; YANG, Y. Influence of Large Reservoir Operation on Water-Levels and Flows in Reaches below Dam: Case Study of the Three Gorges Reservoir. *Sci Rep* 7, 15640. 2017. DOI:10.1038/s41598-017-15677-y.
75. ZHANG, W.; XU, Y.; GUO, L.; LAM, N.; XU, K.; YANG, S.; LIU, K. Comparing the Yangtze and Mississippi River Deltas in the light of coupled natural-human dynamics: Lessons learned and implications for management. *Geomorphology*, v. 399, p. 108075, 2022. DOI: 10.1016/j.geomorph.2021.108075
76. ZHOU, X.; WANG, J.; ZHENG, F.; WANG, H.; YANG, H. An Overview of Coastline Extraction from Remote Sensing Data. **Remote Sensing**, v. 15, n. 19, p. 4865, 2023. DOI:10.3390/rs15194865



Esta obra está licenciada com uma Licença Creative Commons Atribuição 4.0 Internacional (<http://creativecommons.org/licenses/by/4.0/>) – CC BY. Esta licença permite que outros distribuam, remixem, adaptem e criem a partir do seu trabalho, mesmo para fins comerciais, desde que lhe atribuem o devido crédito pela criação original.